

# High surface area anthracene-based microporous polymer bridged by imide links for H<sub>2</sub> storage

Fadi Ibrahim

Department of Chemistry, Abdul Latif Thanian Al-Ghanim School Kuwait, Ardeia, part 6, Fst str, Kuwait.

## ARTICLE INFO

### Article history:

Received: 26 July 2015;

Received in revised form:

28 August 2015;

Accepted: 1 September 2015;

### Keywords

Anthracene,  
Microporous,  
AMP,  
Polymer.

## ABSTRACT

A series of anthracene-based microporous polymers (AMPs) bridged by imide links were successfully prepared by conventional nucleophilic substitution reaction between several 9,10-dihydro-9,10-ethanoanthracenes and cheaper 2,3,5,6-tetrachlorophalonitrile (instead of fluoro-monomer)<sup>1</sup>. AMPs display a BET surface area in the range of 811-988 m<sup>2</sup> g<sup>-1</sup>, and reversibly adsorb 1.59 wt. % H<sub>2</sub> at 1.09 bar/77 K. The enhanced microporosity, in comparison to other organic microporous polymers prepared from (5,5',6,6'-tetrahydroxy-3,3,3',3'-tetramethylspirobisindane)<sup>2</sup> originates from the macromolecular shape of framework, as dictated by the anthracene units, which helps to reduce intermolecular contact between the extended planar struts of the rigid framework. The impressive hydrogen adsorption capture of these materials verified by Horvath-Kawazoe (HK) and NLDFT analyses of low-pressure nitrogen adsorption data.

© 2015 Elixir All rights reserved.

## Introduction

The preparation of purely microporous polymers without the assistance of molecular template is becoming a fast developing area in nonmaterial's research and many approaches have been used to develop various insoluble network organic microporous polymers such as hyper cross-linked polymers (HCP)<sup>1,2</sup>, triptycene-based PIM (Trip-PIM)<sup>3</sup>, conjugated microporous polymers (CMP)<sup>4</sup>, organic framework polymer (OFP)<sup>5</sup>, porous organic polymers (POP)<sup>6</sup> and microporous polyimide networks<sup>7,8</sup> with high specific surface. The most outstanding representation for this kind of materials are the polymers of intrinsic microporosity (PIMs)<sup>9</sup> developed by McKeown and Budd et al with high surface areas in the range of 500-900 m<sup>2</sup>/g.<sup>10, 11</sup> The ideal structure of this ladder polymer result from polycondensation reactions of bisphenols and bi-halo aromatics is a linear unbranched chain free of macrocyclic species and crosslinking. Microporous rigid polymers (AMPs) based on 9,10-dihydro-9,10-ethanoanthracenes monomers bridged by imide links was synthesized efficiently by the double aromatic nucleophilic substitution reaction<sup>1</sup>.

**Comparison between AMP-1 and PIM-PI-1 linear polymer contain the same 2,3,5,6-tetramethyl-1,4-phenylenediamine monomer**

For the polymerization reactions, the choice of aromatic diamine was determined by their previous success as monomers for preparing permeable polyimides. Hence, 2,3,5,6-tetramethyl-1,4-phenylenediamine<sup>12</sup>, 5,5'-(hexafluoroisopropylidene)-di-*o*-toluidine<sup>13</sup> and 2,2'-bistrifluoromethyl-4,4'-diaminobiphenyl)-dianiline<sup>14</sup> monomers were choiced to react with TTSBI to give AMP-1, AMP-3 and AMP-4 polyimids respectively.

The nature of bonding and texture of polymers mainly correlates the microporosity, which could further help to design the polymer based substrate. Although direct comparisons are difficult, it seems clear that networks possess greater microporosity than non-network polymers assembled from similar monomers, presumably due to macrocyclization. The polyimide network AMP-1 (derived from monomers 2,3,5,6-tetramethyl-1,4-phenylenediamine and octahydroxy monomer) has an apparent BET surface area of 995 m<sup>2</sup> g<sup>-1</sup>, whereas that of

the soluble linear polyimide PIM-PI-1 derived from TTSBI monomer and same (2,3,5,6-tetramethyl-1,4-phenylenediamine) monomer<sup>2</sup> (as shown in Figure 1) has only surface area of 600 m<sup>2</sup> g<sup>-1</sup>.

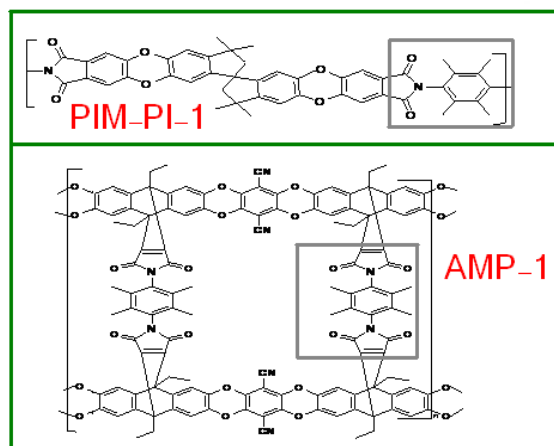


**Figure 1. Structure of AMP-1 polymer and soluble PIM-PI-1<sup>2</sup> polymer based on TTSBI monomer with same 2,3,5,6-tetramethyl-1,4-phenylenediamine monomer.**

## Experimental

### Materials and Methods

All the chemicals were of reagent grade purity and used without further purification. The dry solvent Dimethylformamide (DMF) with water content less than 0.005% was purchased from Aldrich Co. The finely grounded anhydrous potassium carbonate was used after further drying at 200 °C. <sup>1</sup>H-NMR spectrum (400 MHz) of monomers were recorded on a Bruker DPX 400 spectrometer using CDCl<sub>3</sub> as the solvent and tetramethylsilane as the internal standard. Solid state <sup>13</sup>C-NMR measurement was carried out on a Bruker Avance 300 spectrometer equipped with a cross polarization magic angle spinning (CP/MAS) probe and a fully automated pneumatic unit for sample spinning. The specific surface area was calculated using the Brunauer-Emmet-Teller (BET) equation. The micropore area was calculated using *t*-plot method. The pore size distributions were calculated from the adsorption isotherm

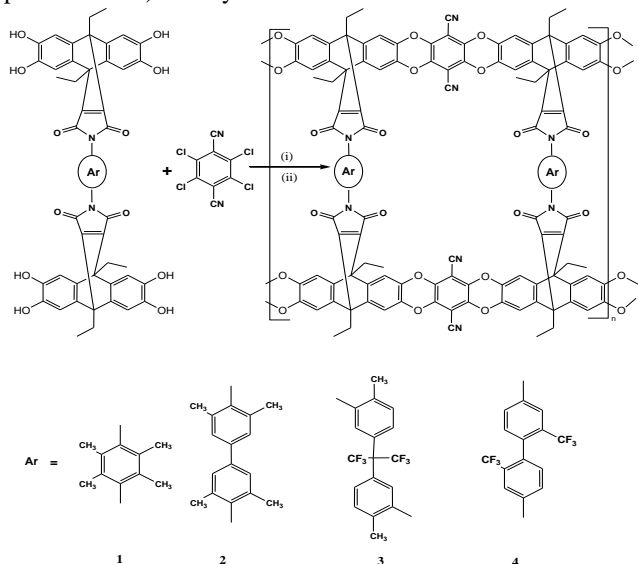
Tele:

E-mail addresses: [fed\\_000@yahoo.com](mailto:fed_000@yahoo.com)

using the Horvath-Kawazoe (H-K) and Nonlocal Density Functional (NLDFT) calculations. The heats of adsorption for  $H_2$  was calculated using the ASAP 2020 software (Micromeritics, Norcross, GA).

### Synthesis of AMPs

Microporous rigid polymers (AMPs) based on 9,10-dihydro-9,10-ethanoanthracenes monomers bridged by imide links was synthesized efficiently by the double aromatic nucleophilic substitution reaction as shown in Scheme 1. This nucleophilic substitution reaction apply dioxane,<sup>14</sup> forming reaction between the corresponding octahydroxy monomers and tetrachloro-terphthalonitrile (instead of tetrafluoro-terphthalonitrile)<sup>1</sup> in dry DMF and 100 °C.



**Scheme 1. Synthetic pathway toward the polyamide network AMP(1-4)s. Reagent and conditions: (i)  $K_2CO_3$ , and DMF (ii) 100 °C for 48h.**

The network polymer was washed with a variety of organic solvents and dried under vacuum. The anthracene based monomers (AMP[1-4]) were prepared in good yield by the straight forward one step imidisation reaction between corresponding anhydride and different amines in refluxing acetic acid. The proposed structure and purity of the obtained monomers were confirmed by routinely spectroscopic techniques as well as elemental analysis (See Supporting Information). The polymers AMP-[1-4]) were synthesized by the dibenzodioxane formation reaction between the tetrol, and tetra-chloroterephthalonitrile in dry DMF as illustrated in Scheme 1. The structures of all prepared AMPs were characterized by FT-IR, solid state  $^{13}C$  NMR spectroscopy and elemental analysis. All materials retained its characteristic stretching bands related to the imide groups ( $C=O$  symmetric and asymmetric stretching in the range of 1722-1792). Moreover it is clear from the spectrum that the base catalyzed polymerization condition does not make any destruction in the imide units (See Supporting Information). The  $^{13}C$  NMR spectra of the AMPs were fully consistent with their proposed structures (See Supporting Information). The signals originating from the hydroxyl groups of tetrol were disappeared, suggesting that the reaction was carried out completely through dibenzodioxane formation. The broad aromatic and aliphatic signals of AMPs were enough to confirm the formation of high molecular weight polymers. The thermal properties were evaluated by TGA and DSC. The decomposition temperatures were also very high; where a 5-10 % initial loss around 400 °C, were observed, corresponding to the vaporation of the residual solvents which has been identified as the entrapped solvents in the micropores

used for processing the sample. The good thermal stability can be attributed to its double stranded structures. In DSC analysis no melting ( $T_m$ ) and glass transition ( $T_g$ ) was observed. Wide Angle X-ray Diffraction (WAXD) analysis of the AMPs was conducted to display no crystalline peaks and revealed that all the prepared materials were amorphous.

### Structure-property relationship

Different spacers have been employed in order to evaluate the structure feature on surface area. The anthracene groups as thermally and oxidatively stable, rigid moiety can improve physical properties such as enhanced thermal stability, increased chain stiffness, and decreased crystallinity.<sup>15</sup> However, for AMP-1 there is very highly restricted rotation about the imide bond linkages, giving rigidity to the polymer. In AMP-2, there is potentially more flexibility in the backbone, but the hexafluoroisopropylidene unit provides a kink in the chain and may be regarded as an additional site of contortion. The unique shape of the anthracene unit lead to a rigid network structure composed of nanoporous frameworks. The molecular structures of these PIM-polyimides have features of the spiro-center providing a site of contortion as well as having conventional imide linkages, this results a very highly restricted rotation about these bonds, giving rigidity to the polymer. The shape of this monomer constrains the growth of the polymer within the same plane to provide a rigid macromolecular structure with large concavities. The faces of the ribbonlike "struts" between the anthracenes are oriented nearly perpendicular to the plane of the macromolecular growth. This arrangement blocks face-to-face association between these planar struts, leading to greater IM. For the attainment of microporosity in network polymers, it appears that the requirement for the prevention of rotation about single bonds is unperturbed, presumably due to the network itself preventing structural rearrangement that could result in a collapse of the porous structure. Hence, the formation of rigid amorphous network polymers using anthracene monomer is compatible with obtaining highly microporous materials. Perhaps the clearest demonstration of IM is found for well defined rigid oligomers containing triptycenes as the concave unit. An interesting structure-property relationship is evident for these materials in that the longer the linear struts between the branch points, the lower is the porosity. And is likely related to a larger number of bonds with rotational freedom, which will reduce IM.<sup>10</sup>

### Nitrogen adsorption analysis

Nitrogen adsorption measurements of AMPs where measured, for example, the BET surface area of AMPs is relatively high, which is higher than the Trip-PIM<sup>16</sup> but less than the HCPs<sup>17</sup> as shown in Figure 2.

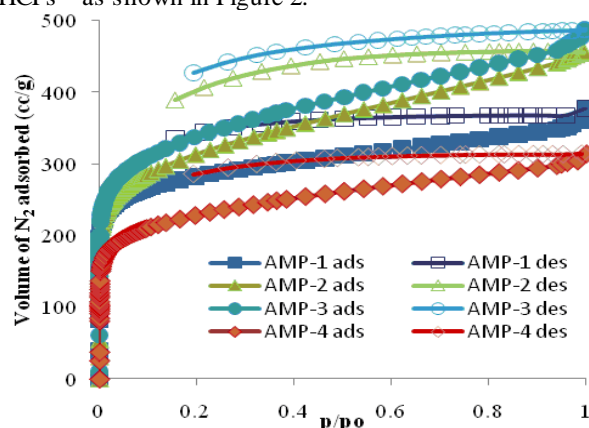


**Figure 2. Nitrogen adsorption/desorption isotherm at 77 K for AMPs**

**Table 1.** <sup>a</sup>BET surface area of AMP (1-4)s calculated from nitrogen adsorption isotherm.

PIMs	SA <sub>BET</sub> (m <sup>2</sup> /g) <sup>a</sup>	PV <sub>micro</sub> (cm <sup>3</sup> /g)	HK/NLDFT pore width (Å <sup>c</sup> )	SA <sub>LAN</sub> (m <sup>2</sup> /g) <sup>b</sup> (77K / 87K)	H <sub>2</sub> (wt.%) at 1.13 bar, (77K/87 K)	Q <sub>st</sub> (kJ/mole)
AMP-1	995(796)	0.45	5.56 /6.29	663/523	1.59/1.23	7.19
AMP-2	956(705)	0.52	5.43/6.64	343/275	1.52/0.63	6.99
AMP-3	988(869)	0.41	10.8/6.67	467/353	1.77/1.43	7.70
AMP-4	811(716)	0.39	8.4/6.66	531/436	1.18/0.92	6.85

The adsorption/desorption isotherms clearly exhibit pronounced hysteresis up to low partial pressure, which is typically observed for microporous materials. Nitrogen uptake increases in the sequence AMP-4 < AMP-1 < AMP-2 < AMP-3,<sup>1</sup> this is reflected in the results of analysis by the (BET) method, which gave apparent surface areas of 811, 988, 856, and 995 m<sup>2</sup>/g respectively

### Hydrogen adsorption

The main task is finding the potential of the prepared materials in storing considerable amount of hydrogen. For example, the hydrogen storage quantities for AMP-1 in a pressure range 0-100 bar (as shown in Figure 3) increase gradually with pressure increase. The isotherms are fully reversible and exhibit a sharp rise at low pressure region which is consistent with the physisorption of hydrogen on a microporous material. All the prepared AMPs show similar behaviors in their isotherm with a significant uptake at two different temperatures (Table 1).

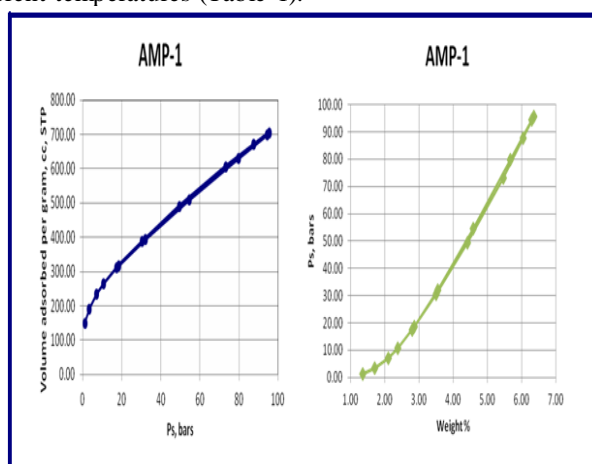


**Figure 3.** High pressure H<sub>2</sub> adsorption capacity of AMP-1 (0-100 bar)

The Langmuir isotherm theory assumes monolayer coverage of adsorbate over a homogenous adsorbent surface of equal energy. The isosteric heat of adsorption, (Q<sub>st</sub>), for dihydrogen molecules on all samples was calculated from the adsorption isotherms at 77 and 87 K as shown in Figure 4. The chemical nature of the accessible surfaces and morphology of the pores have thus to be tuned to enable a high adsorption enthalpy. It has been already known that microstructure had a deep impact on hydrogen uptake which is further influenced by the geometry of the building units. So materials containing high electron rich sites were found to increase the hydrogen adsorption enthalpy. The combination of microporosity and chemical functionality of these AMPs are very promising for applications in the air purification, or separation. As compared to MOFs and similar metal containing porous structures, the concept of preparing hydro-thermally stable AMPs having organic spacers along with predefined functionality allows them to extend in many adsorption applications.

In order to attain good storage capacity, it will be necessary to design materials with greater accessible surface area and microporosity. The hydrogen adsorption isotherm measured at 77 K and 87 K and the calculations involve the Langmuir equation and *t*-plot analysis. This methodology avoids the problem of over counting the nanopores that is associated with the specific surface area measured by nitrogen adsorption. Figure 4 shows the hydrogen adsorption/desorption isotherms of AMP-1.

The number in the parathesis is the micropore surface area calculated using the *t*-plot analysis. PV<sub>micro</sub> is the micropore volume. <sup>b</sup>Surface area calculated from the H<sub>2</sub> adsorption isotherm using Langmuir equation at 77 K and 87 K. The storage capacity of a physisorption-based hydrogen carrier is the sum of the capacity.

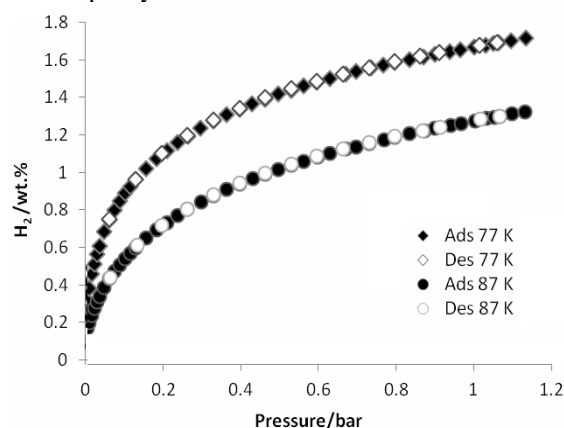


**Figure 4.** Adsorption/desorption isotherms at 77 and 87 K for AMP-1.

In addition, the adsorption is completely reversible and there is no significant hysteresis which can be correlated with the physisorption of hydrogen on a microporous material. The repeatability of the hydrogen adsorption was also checked and found to be constant even after the repeated cycles. The shape of the isotherm indicates that adsorption has not reached saturation and further significant hydrogen uptake could occur at higher pressures. The framework OFP-3 afforded a hydrogen storage capacity of 1.43 wt% at 1 bar and 87 K, which is comparable with the other reported microporous polymers. However, at 77 bars AMP-3 adsorbs nearly 1.77 wt% by weight of material.

### Pore size distribution

The pore size distribution calculations show subnanometer pores. The enhanced microporosity, in comparison to other organic microporous polymers<sup>16</sup>, originates from the rigid and nonplanar structural units, which helps to reduce intermolecular contact between the extended planar struts of the rigid framework. Small sub nanometer pores ranging from 0.5 to 0.6 nm (as shown in Figure 5) are the most efficient for hydrogen sorption while mesopores decrease volumetric capacity and contribute little to storage capacity. The hydrogen adsorbs readily at relatively low pressure.

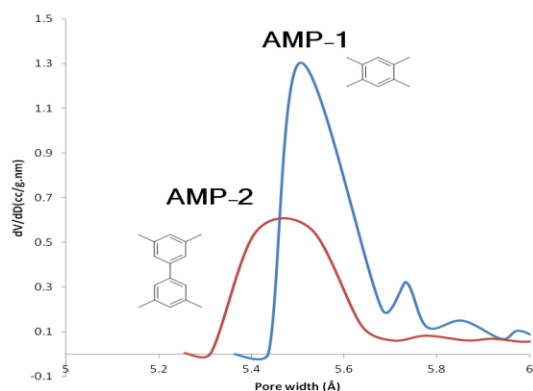


**Figure 5. Micropore size distribution calculated by HK method of AMP-1 and AMP-2**

The faces of the ribbonlike<sup>17-19</sup> “struts” between the TTSBI units are oriented perpendicular to the plane of the macromolecular growth. This arrangement blocks face-to-face association between these planar struts, leading to greater IM. Figure 6 demonstrate the micropore size distribution (MPSD) as calculated by the (HK) method. Our MPSD analyses for all AMPs are in the range of 0.48-0.59 nm.

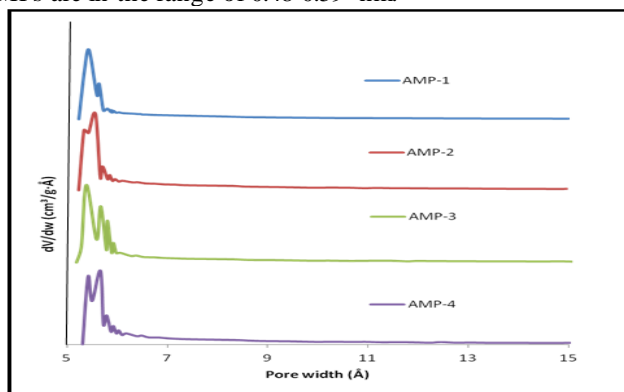


**Figure 6. Pore size distribution for AMP(1-4)s, calculations using HK calculations clearly shown the presence of ultra micropores**

### Synthesis of AMP-3

To a solution of octahydroxy-anthracene (0.2 g, 0.21 mmol) and 2,3,5,6-tetrachlorophalonitrile (0.08 g, 0.43 mmol) in dry DMF (40 ml), K<sub>2</sub>CO<sub>3</sub> (0.35 g, 2.52 mmol) was added and heated to 100 °C for 48 h. Then, the reaction mixture was allowed to cool and precipitated in acidified water. The precipitate was filtered off and washed with deionised water and then with methanol. The purification was done by washed repeatedly with THF and methanol. The resulting AMP-3 is brown solid and dried in vacuum at 80 °C for 12 hrs (yield 80 %).

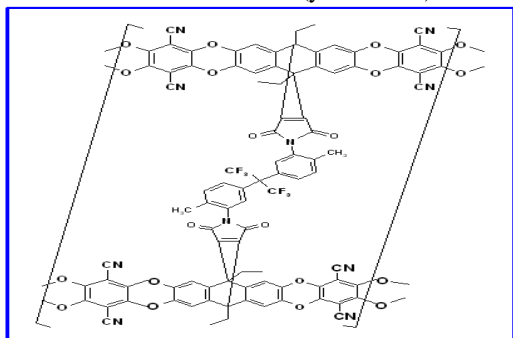


**Figure 7. AMP-3**

Yield 85%; mp. > 300 °C; MS (EI): m/z (%) 1851(M<sup>+</sup>). IR/cm<sup>-1</sup> (KBr): 1788 (asym C=O, str), 1722 (sym C=O, str), 1366 (C-N, str), 744 (imide ring deformation). <sup>13</sup>C NMR (100 MHz): 169.7, 148.7, 145.3, 142.8, 141.5, 139.5, 138.2, 128.8,

121.6, 123.8, 115.8, 115.2, 104.6, 109.2, 55.8, 55.5, 42.9, 39.6, 15.5, 10.3, 8.6. CHN Calculated for C<sub>105</sub>H<sub>80</sub>F<sub>6</sub>N<sub>10</sub>O<sub>16</sub> (1851): C 68.02; H, 4.32; N, 7.56. Found: C, 67.70; H, 4.21, N, 7.22. BET surface area = 988 m<sup>2</sup>/g; total pore volume = 0.41 cm<sup>3</sup>/g.

### Acknowledgments

I'm grateful for the facilities from ANALAB in Kuwait university and dr.Sadd Makhseed.

### Conclusions

Anthracene-based microporous polymers bridged by imide links (AMPs) was synthesized efficiently by the dioxane forming reactions using cheaper chlorinated monomer instead of fluorinated. AMPs display a BET surface area reach to 988 m<sup>2</sup> g<sup>-1</sup>, and reversibly adsorb reach to 1.77 wt. % H<sub>2</sub> at 1.13 bar 77 K. The isotheric heat of adsorption about 7.4 kJ/mole. The enhanced microporosity, in comparison to other organic microporous polymers, originates from the macromolecular shape of the framework, as dictated by the triptycene units.

### References

- [1] Saad Makhseed and Jacob Samuel *J. Mater. Chem. A*, 2013,1, 13004-13010
- [2] Fadi Ibrahim. *Elixir Nanocomposite Materials* 62, 2013,17542-17548
- [3] Saad Makhseed, Fadi Ibrahim, Jacob Samuel. *Polymer*. 53, 2012, 2803-3052.
- [4] Ghanem, B. S.; McKeown, N.B.; Harris, K.D.M.; Pan, Z.; Budd, P.M.; Butler, A.; Selbie, J.; Book D.; Walton, A. *Chem Commun* 2007, 67-69.
- [5] Jiang, Jia-X.; Su, F.; Trewin, A.; Wood, C. D.; Campbell, N. L.; Niu, H.; Dickinson, C.; Ganin, A.Y.; Rosseinsky, M. J., Khimyak Y.Z.; Cooper A.I. *Angew Chem Int Ed.* 2007, 44, 8574-8578.
- [6] Makhseed S.; Samuel. *J. Chem Commun*, 2008, 4342- 4344.
- [7] Yuan, S.; Dorney, B.; White, D.; Kirklin, S.; Zapol, P.; Yu, L.; Liu, Di-J. *Chem Commun*, 46, 2010, 4547- 4549.
- [8] Wang, Z.; Zhang, B.; Yu, H.; Sun, L.; Jiao, C.; Liu, W. *Chem Commun*. 46, 2010, 7730-7732. 683.
- [9] McKeown N. B.; Budd P. M. *Chem Soc Rev*, 2006, 35, 675-680.
- [10] Budd, P. M.; Ghanem, B. S.; Makhseed, S.; Mckeown, N. B.; Msayib, K.; Tattershall, C. E.; Wang, D. *Chem Commun*, 2004, 2, 230-23
- [11] Bader S. Ghanem, Mohammed Hashem, Kenneth D. M. Harris, Kadhun J. Msayib. Mingcan Xu. (2010). 43: 5287-5294.
- [12] Quanyan Z., Shenghai Li, Wenmu Li, Suobo Z. (2007). *Polymer*, 48: 6246-6253.
- [13] Raf G., Mario S., Wim D. 2002. Brosted-and Lewis acid-catalyzed cyclization giving rise substituted anthracenes and acridines. 43: 6605-6608.
- [14] Ghanem BS, Msayib KJ, McKeown NB, Harris KDM, Pan Z, Budd PM, Butler A, Selbie J, Book D, Walton A. (2007). *Chem Commun*, 67-69.
- [15] Colin D. Wood, Bien Tan, Abbie Trewin, Hong Jun Niu, Darren Bradshaw, *Matthew J.* (2007),19: 2034-2048.
- [16] Jiang J-X, Cooper A. (2010). *Topics Curr Chem*, 293:1-33.
- [17] D. Hofman, J. Ulbrich, D. Fritsch, D. Paul. 1996, *Polymer*, 37: 4773-4785.
- [18] H.S. Kim, Y.H. Kim, S.K. Ahn, S.K. Kwon. 2003, *Macromolecules*, 36, 2327-2332.
- [19] Yongli Mi. Takuji Hirose. 1996. *Journal of polymer research*, 3: 11-19.